Strengthening Road Pavement Concrete By Combining Crumb Rubber With SFRC Fibers

Ali Al-kanaani* and Sepanta Naimi

Faculty of Engineering and Natural Sciences, Department of Civil Engineering, Altınbaş Üniversitesi, Bağcılar 34217 İstanbul, Turkey

**Corresponding author. E-mail: Alikanaani2020@gmail.com*

Received: Jan. 30, 2023; Accepted: Apr. 21, 2023

Improving concrete pavement structure is a primary objective utilized to improve road pavement performance. The effect of crumb rubber and steel fiber is to protect and strengthen the strength of reinforced pavement concrete. In this study, experimental work was conducted utilizing a concrete model to examine reaction and resistance to the effect of carloads. The experimental laboratory program was divided into four groups: standard concrete and concrete with crumb rubber, SFRC, and combined crumb rubber and SFRC. the results observed that the addition of 10 to 20% crumb rubber and 40% SFRC to concrete with an fc of 30 MPa significantly improves the concrete's behavior under the same conditions. Additionally, the crumb rubber and SFRC shear strength enhanced in comparison to concrete characteristics.

Keywords: Crumb rubber, SFRC, Concrete Pavement, Stress, Mechanical characteristics

http://dx.doi.org/10.6180/jase.202406_27(6).0006

---

1. Introduction

A large quantity of solid trash has been produced as a result of worldwide industrialization and technological progress. As a result, 1.5 billion tires are thrown away every year, a practice that exacerbates environmental damage. It is the responsibility of scientists, engineers, researchers, and governments to create low- or no-cost, high-efficiency methods of waste management, such as plastic waste recycling. These strategies should also include the recycling of waste products for applications like road building, which would have positive effects on the environment. Because of this, several researchers are looking for ways to improve the recycling of flexible garbage. There are many positive outcomes associated with well-managed trash reuse [1]. In fact, many types of plastic debris, including polyethylene terephthalate (PET), low-thickness polyethylene (LDPE), high-density polyethylene, and polyethylene, are employed as pavement preservation agents. The disposal of these assets has become a severe concern due to the rising global consumption of plastic containers and bottles every year from the wealthiest to the poorest countries [2]. Government-funded highway construction projects in the United States and France have mandated the usage of rubber in crumb states [3, 4]. Research into the impact of tires on concrete's resistance with freeze and thaw consideration has been conducted by Benazzouk and Queneudec [5], Paine, Dhir [6], Savas, Ahmad [7]. In the end, they determined that rubber could be useful as an agent in concrete considering freeze-thaw, as it improved the durability of the mixture compared to untreated concrete. Crumb tire rubber used for HSC for structural purposes has been shown to increase the material's resilience to fire and decrease spalling damage caused by flames by Hernandez-Olivares and Barluenga [8]. Other elements of structures, including culverts, walkways, running tracks, crash barriers, sound absorbers, etc., can all benefit from the usage of rubberized concrete, according to the writing of Yang, Kjartanson [9]. More recently, research on the Tunisian tire market conducted by a former senior customs official believes that the informal sector today controls 73% of the market in Fig. 1.

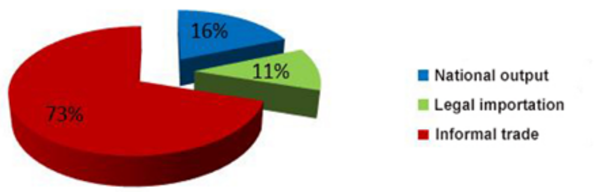

Fig. 1. Distribution of Demand for Tires [10].

Given the lack of tire data and accurate statistics on the fleet of vehicles on the road, such an estimate raises issues. However, the number of vehicles on the highway is multiplied by the coefficient of annual consumption for each kind of vehicle used to identify the country's tire demand [11]. The shredded rubber was separated into two sizes, ranging from 5 to 10 millimetres and 10 to 20 millimetres in diameter, depending on the size of the chips. Rubber grains of both sizes were dispersed uniformly. The rubber particles can vary in size from 1 millimeter to 5 millimeters [12].

The product would be better characterized as aggregate rubber because the dry process does not suit the traditional description of asphalt-rubber binders [Anderson et al., 2000]. Another researcher Sebaaly, Gopal [13] demonstrates that adding rubber to binders with asphalt improves their viscous-elastic characteristics. De-vulcanization procedures, including thermo-mechanical (including those aided by supercritical CO_2 and devulcanizing chemicals), chemical, ultrasonic, microwave, and biological, represent a significant advancement in the recycling of rubber from ELT [14–16]. The degree of de-vulcanization and the selectivity (i.e., the ratio between cross-links breakdown and chain scission) achieved through thermo-mechanical approaches are sensitive to various factors and processing parameters. Dierkes, Dijkhuis [17], Macsiniuc, Rochette [18], Saiwari, Van Hoek [19] considered the rubber matrix playing a pivotal role in determining the optimal conditions for both. Due to their complex composition, which includes natural rubber (NR), styrene-butadiene rubber (SBR), butadiene rubber (BR), and halobutyl rubber, fillers (silica modified with silane and/or carbon black), oils, and other ingredients sourced from various areas of the tire (such as the tread, inner liner, and sidewall), the quality of devulcanized products derived from ELT is limited [19]. In recent years, it's been shown that other types of fiber are suited for concrete structural components and perform similarly [20]. To create fiber-reinforced concrete, strands of fiber are mixed into the concrete mix. The strength and crack pattern of concrete are both enhanced by the addition of fibers. Instead of just one or two large cracks, fiber-reinforced concrete tends to show off a slew of smaller ones [21]. The global average annual consumption of plastic has increased from roughly 5 million to 100 million tons throughout the last half-century. So, plastic has emerged as one of the last several decades' most notable solid waste products [22]. Polymers, sometimes known as sludge asphalt mixtures, can be used in a wide range of civil engineering and building projects [23].

Concrete reinforcement with the use of fibers is commonplace and is governed by the fib Model Code 2010. The main benefits include optimizing execution times by eliminating prestressed reinforcement in part or in whole and increasing the post-cracking energy of the concrete, which results in better-cracking patterns that prolong the life of the building [24, 25]. Fibre-reinforced concrete (FRC) is commonly used for tunnel lining rings and sewage pipes [26, 27], and it has been demonstrated that using FRC in place of standard passive reinforcing fibers improves sustainability in both contexts in measurable ways. Self-compacting concrete not only speeds up production but also decreases the likelihood of voids and other finishing problems that can produce aesthetic faults or even impair the durability of the construction, among other benefits. All of these extras help make the final product more long-lasting.

A good pavement will be thick enough to safely transfer wheel weight loads to the sub-grade soil and have a solid structural foundation [28]. The base courses of a flexible pavement should be solid and durable. In spite of the intense stresses exerted by the road surface, these high-quality materials will hold up well [29].

There are three unique uses for fiber reinforcement in concrete structures. A one-dimensional random distribution increases the fibre's shear resistance and crack control. Table 1 displays the distribution of SFRC percentages among normal-weight individuals [30]. In 1913, Talbot presented a foundational model for the punching behavior of reinforced concrete [31] based on the results of the first experimental inquiry into the problem. The research aimed to determine the causes of footing cracks and deflection in concrete. The failure loads of each footing were also determined [32]. Steel fibers can be purchased in several different configurations, including round, rectangular (0.3 to 0.5 mm thick), and deformed bundles. There are two types of fibers utilized in this process: shorter fibers are used to prevent cracking, while longer fibers are used to create a strong bond between the fibers and the concrete. The blend can be designed to suit a specific application [33].

Table 1. Explanation of the experimental protocol.

Specimen	Concrete Type
ALI 1 P	Concrete (control)
ALI 2 R10	10% Crumb Rubber with Concrete
ALI 3 R20	20% Crumb Rubber with Concrete
ALI 4 S	60% SFRC with Concrete
ALI 5 RS	60% SFRC, 10% Crumb Rubber with Concrete
ALI 6 RS	60% SFRC, 20% Crumb Rubber with Concrete

2. The aim of this study

The aim of this study is to strengthening concrete pavement by adding crumb rubber combine with SFRC. The main steps to achieve the targets are:

i. To investigate the mechanical properties of the concrete with crumb rubber of tires.

ii. To evaluate the mechanical properties of the concrete with crumb rubber of tires and different amount of SFRC component.

3. Materials and methods

The detailed FEM model for the panels was created utilizing the ANSYS Finite Element program's routines and nonlinear elements to simulate the related forces. This model provides the foundation for the numerical analysis of the panels. The finite element method (FEM) is commonly used in civil engineering and other technical disciplines. This chapter describes how the study evaluated the behavior of concrete containing different percentages of Crumb Rubber and how laboratory data was incorporated into an ANSYS tool to analyze panel behavior at various temperatures. This chapter explains the techniques used to replicate the behavior of the panel. The panel will be subjected to a variety of loads dependent on its form, size, and applied reinforcing kinds. The model will be evaluated with a technique that discretizes partial differential equations into small control volumes known as meshes and cells. Kubaisa cement was employed in this investigation, which was procured from western Iraq. Because the workability of the intended combination is too low owing to the high percentage of fine aggregate, a high water reducer is utilized in a consistent percentage for all mixtures. Sika's conventional superplasticizer is employed, and it complies with ASTM C 494 Types A and B [34]. Fine aggregate is graded river sand sourced locally.

i) aggregate particles sizes ranging from 0.075 mm to 4.75 mm were utilized.

ii) the diameter of SFRC is ranging from 0.25 mm to 0.75 mm.

iii) the rubber particle size is ranging from 1 mm to 3 mm.

To get a homogenous mixture, the components were blended. The used rubber crumbs has been illustrated in Fig. 2. The water is progressively added to the mixture, followed by the superplasticizer, and finally, the RUBBER. The mixture is ready for casting shortly after adding the rubber. As illustrated in (Fig. 3), the mold was carefully greased to prevent the concrete from adhering to it and to make it easier to retrieve the sample.

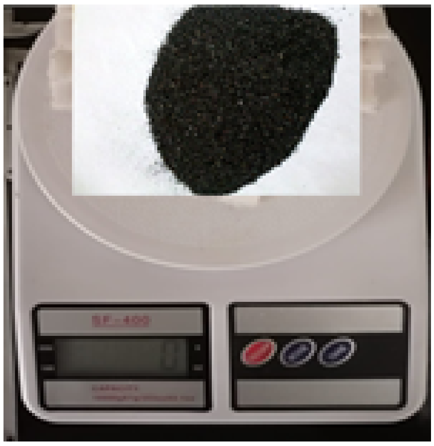

Fig. 2. The Used Rubber Crumbs.

Fig. 3. The cubic of the present study samples.

Then the concrete is poured into the mold using a vibrator, exterior vibration for the samples, and cubic. The sample was placed in a water tank with a heater to begin the curing process at a temperature of 25 degrees Celsius, where it remained for 28 days. Table 1 shows the specimen title and concrete type.

Since the volume percentage of crumb rubber fiber reinforcement is a crucial variable, both unreinforced and reinforced concrete samples were subjected to testing. Twelve distinct simulation tests may be conducted. After the material had cured for 28 days, a basic compressive resistance was utilized to calculate stresses. The modulus of elasticity was determined by correlation using this set of stresses (MPa). Typically, the f′c values at 28 days for concrete used in rigid pavement are 30 MPa.

4. Results and findings

4.1. Lab Experiment Results

Cubic's testing took place on the same day as the samples test. Fig. 4 depicts the test machine for all cubic tests. Describes the process for estimating concrete cubic compressive strength. A compressive axial load must be applied to the sample once it has been prepared and placed in the crest of the machine until failure occurs. The experimental approach is detailed in detail below. Cement begins to harden immediately upon contact with water. This hardening is the consequence of a process referred to as crystallization. The formation of crystals and their subsequent interlocking occurs following the expiration of an initial period. Before the cement has a chance to set, concrete is completely fluid, and it gradually hardens afterward.

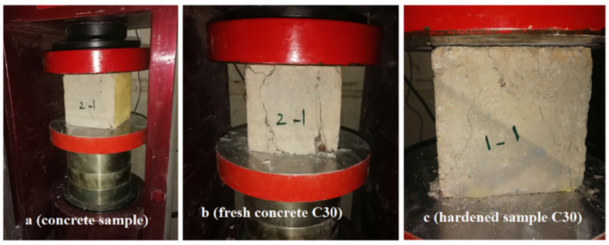

Fig. 4. The laboratory tests.

Due to the significance of the volume proportion of fiber reinforcement in the overall composition, experiments were conducted on both "control" and "fiber reinforcement" concrete. Because the volume percentage of crumb rubber fiber reinforcement is a crucial variable, testing was conducted on both "control" and "crumb rubber fiber reinforcement" concrete. Stresses were computed after a 28-day recuperation period, and fundamental compressive resistance was a significant factor. After the curing process was complete, this durability was considered. Using these pressure measurements and a matching technique, we were able to estimate the modulus of elasticity of the material (MPa). After 28 days, f′c values of 30 MPa are more the rule than the exception for rigid pavement concrete.

The given data (Table 2) presents the compressive strength of six different specimens of concrete, all tested after 28 days of curing. The first specimen, ALI 1 P, is the control group, with no additives or modifications, and has a compressive strength of 31.45 MPa. The second and third specimens, ALI 2 R10 and ALI 3 R20 respectively, have rubber added to the concrete mixture in the amounts of 10% and 20%. Both of these specimens exhibit lower compressive strengths than the control group, with ALI 2 R10 having a compressive strength of 25.52 MPa and ALI 3 R20 having a compressive strength of 23.52 MPa. The fourth specimen, ALI 4 S, has 60Kg/m^3 of steel fiber reinforced concrete (SFRC), resulting in a compressive strength of 33.67 MPa, which is higher than the control group. The final two specimens, ALI 5 RS and ALI 6 RS, are also SFRC, but with the addition of rubber in the amounts of 10% and 20%, respectively. These two specimens have compressive strengths of 30.9 MPa and 28.36 MPa, both of which are lower than the SFRC-only specimen but higher than the rubber-only specimens.

Typically, the f′c values at 28 days for concrete used in rigid pavement are 30 MPa. This study examines various resistances in that range, as well as thicknesses up to 200 millimeters thick. Table 3 shows the variation in strength using various percentages of rubber crumbs in the mix.

The data that is represented in Table 3 is the edge stress of five different specimens of concrete subjected to different load levels. The specimens are all C30 grade, and they have varying percentages of rubber and steel fiber reinforced concrete (SFRC) added to them. The first two specimens, C30 with 10% rubber and C30 with 20% rubber, have compressive strengths of 1.91 MPa and 2.26908 MPa respectively under a load of 100 KN. The addition of rubber results in a slight increase in edge stress compared to the control group. However, as the load level increases, the edge stress of the rubber-added specimens surpasses that of the control group. The third and fourth specimens, C30 with 60 kg/m^3 SFRC and C30 with 60 kg/m^3 SFRC with 10% rubber, have compressive strengths of 1.729696 MPa and 1.94056 MPa respectively under a load of 100 KN. The addition of SFRC results in a reduction in edge stress compared to the control group. However, as the load level increases, the edge stress of these specimens surpasses that of the control group. The fifth specimen, C30 with 60 kg/m^3 SFRC with 20% rubber, has a compressive strength of 2.2156 MPa under a load of 100 KN, which is higher than the SFRC-only specimen but lower than the rubber-only specimens.

Table 2. The compressive test results.

Specimen	Compressive Strength of Concrete (28 days)	f'c (MPa)
ALI 1 P	compressive strength of concrete	31.45
ALI 2 R10	compressive strength of concrete with 10% rubber	25.52
ALI 3 R20	compressive strength of concrete with 20% rubber	23.52
ALI 4 S	compressive strength of concrete with 60 Kg/m^3 SFRC	33.67
ALI 5 RS	compressive strength of concrete with 60 Kg/m^3 SFRC with 10% rubber	30.9
ALI 6 RS	compressive strength of concrete with 60Kg/m^3 SFRC with 20% rubber	28.36

Table 3. Compressive strength with the load variation.

Load (KN)	Edge Stress (MPa)	C30 with 10% Rubber	C30 with 20% Rubber	C30 with 60 kg/m^3 SFRC	C30 with 60 kg/m^3 SFRC with 10% Rubber	C30 with 60 kg/m^3 SFRC with 120% Rubber
100	1.91	2.26908	2.5021	1.729696	1.94056	2.2156
150	2.734	3.247992	3.58154	2.47591	2.777744	3.17144
200	3.318	3.941784	4.34658	3.004781	3.371088	3.84888
250	3.9	4.6332	5.109	3.53184	3.9624	4.524

4.2. Model Validation

Before evaluating the concrete pavement model, it is necessary to characterize the characteristics of the concrete and any other components. It is an essential component of the modeling process that ensures that the results are accurate representations of the model's behavior. The main geometry was with length equal to 3.75 m, width equal to 3.75 m and thickness 0.2 m as shown in the Fig. 5.

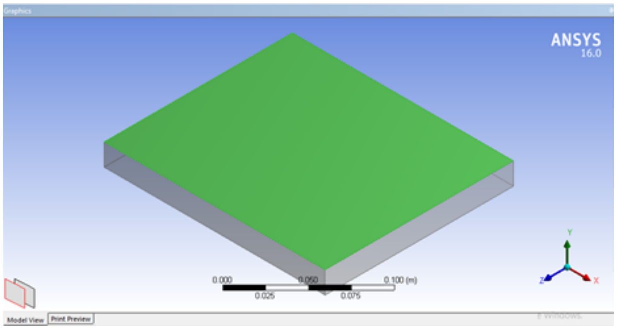

Fig. 5. The main pavement geometry.

The validation and verification of the research are described in this part. The models in this work are evaluated using the collected experimental data. A suitable model with the proper model configuration and mesh technique that can be built and applied to the pertinent boundary condition is selected. This study demonstrates how to construct an accurate model and comprehend the behavior of concrete based on slab models. The validation technique compares the findings of the simulation model to those of a specified model to ensure that the structural simulation model is developed with the correct settings and will be solved in a manner that is a decent approximation of reality.

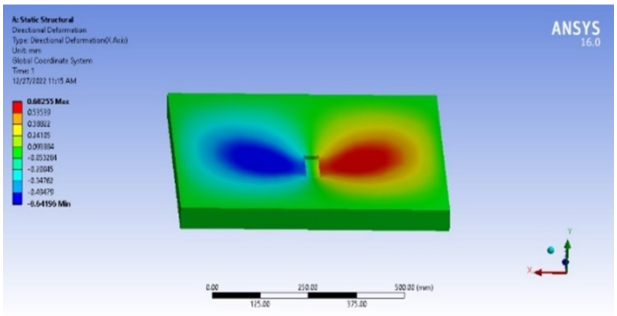

Fig. 6. The ANSYS result based on the study boundary conditions.

The researcher utilized Gherbi's et laboratory experiment findings in 2018 as a model for validation (Fig. 7). In order to measure the slab's center deflection, numerous loads were applied to the center of a two-way slab to acquire the experimental data. The numerical outcomes are contrasted with those determined by Gherbi et al. at room temperature. The results of the simulation demonstrate the similarities and differences between the results of ANSYS tests conducted with the same configuration and those obtained from independent numerical laboratories. The increasing displacement numbers show that the model is correct in every case.

Examining what role crumb rubber plays is an important part of this research. Important because it will be used to evaluate various crumb rubbers' effectiveness. This step cannot be skipped. It was determined that running the ANSYS solver on a three-dimensional concrete slab was

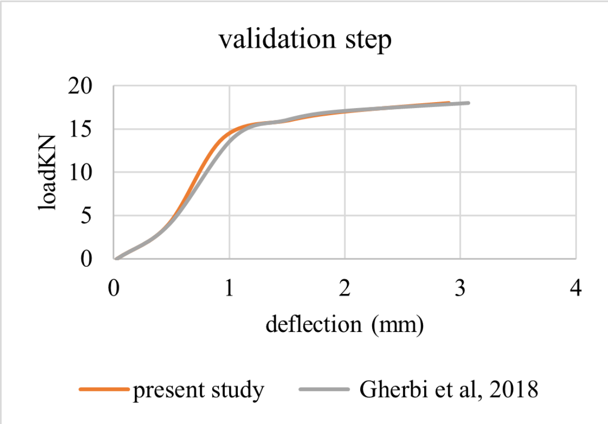

Fig. 7. The validation results.

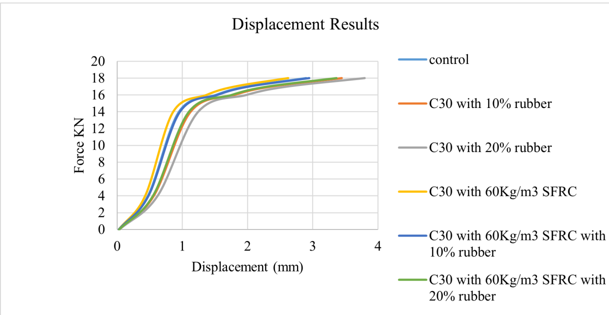

Fig. 8. The displacement results of the sample.

the best independent scenario for accomplishing this goal. We used the slab's geometric midpoint to determine the load-deflection curves. Geometric changes, like deflection and failure, are measured by employing the ANSYS system. These quantities can be linked to information about forces and motions, permitting the establishment of a causal relationship between the two sets of quantities. The force-displacement responses of all investigated slab models are compared across various ANSYS diagrams. The primary purpose of this research was to analyze and propose a novel model for punching shear of concrete slabs reinforced with steel or carbon fiber-reinforced (crumb rubber and SFRC) bars. Here, we provide a formula for determining the shear value of concrete, which can be used to model the expected stress at failure. Several loading quantities were used for the case of room temperature. The figure shows the results of the crumb rubber, SFRC, and concrete slab models. The images display the outcomes of a three-dimensional finite element analysis of the effects of a wheel loader on a jointed plain concrete pavement. The figures present four distinct permutations of pavement material features. One way to examine vertical surface deflection is to plot the change in the top surface of the concrete slab against the distance from the centerline of the circular loaded region along the longitudinal direction of the pavement. Fig. 8 shows the displacement results of the samples. In both the linear elastic analysis and the nonlinear finite element analysis, the maximum vertical surface deflection of the concrete slab at the center of the circular wheel load is 2.899 millimeters. As one approaches the edge of the pavement in the same direction as the concrete, its number drops.First, a volume for the concrete body must be constructed after entering the concrete body's dimensions to simulate a concrete pavement. Steel supports and reinforcements may be modeled simply for the FE analysis since their geometries are mirror images of one other. This is because their geometry is perfectly complementary to one another. The typical tire load and the displacing properties of concrete pavement are also depicted here. The forces of gravity, hydrostatic pressure when the reservoir is at full capacity, and tire pressure all put the model through its paces. Hydrostatic force is applied uniformly along the entire height of the concrete pavement once the model has been self-weighted. This is done as the virtual treads of the tires continue to move across the virtual ground. The load-displacement curves for all tested concrete pavements exhibit the same behavior. The Figures demonstrate the variations seen in the FE Model study between a regular concrete pavement and an SFRC and Rubber reinforced concrete pavement (Figs. 9 and 10). The evaluated concrete pavement's load-displacement curves all follow the same pattern. Every single one of the FE numerical models has a large discrepancy between the final step and the experimental results.

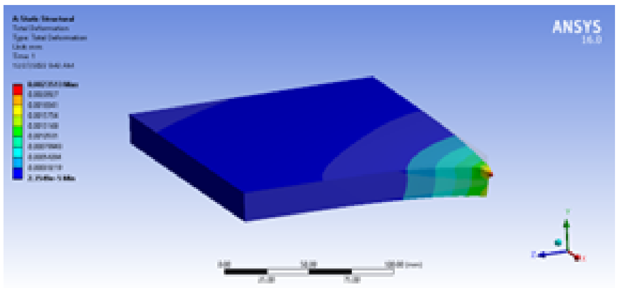

Fig. 9. The displacement results of the sample.

The ANSYS models differ slightly from the model, despite both employing the same numerical technique (FEM). However, the discrepancies are much smaller. A mathematical link between the two factors was employed to lessen the disparity between them, as the resistance in the foundation soil is not always given by the same parameter (in one example, the modulus of elasticity, E, is utilized, and in the other case the response module, k). The resistance in the foundation soil is not determined by the same parameter,

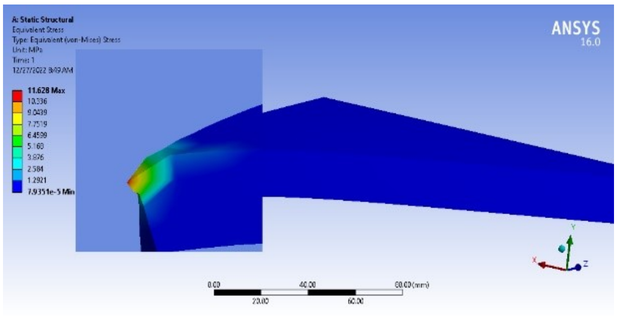

Fig. 10. The displacement results of the sample.

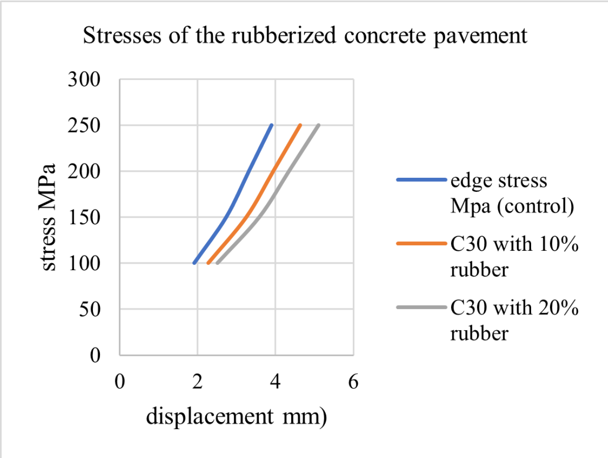

Fig. 11. The displacement results of the sample.

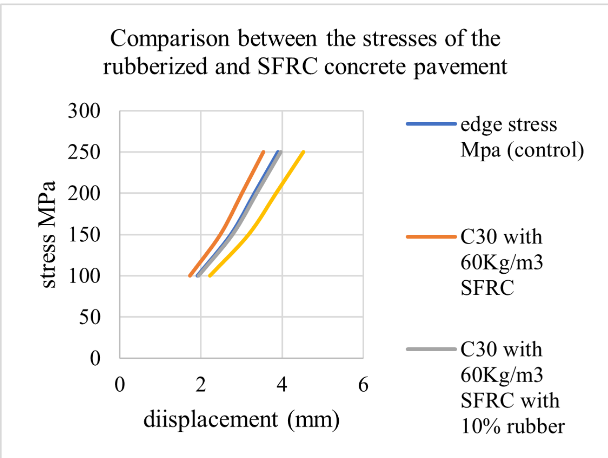

Fig. 12. The displacement results of the sample.

and they experience different physical phenomena, therefore, these variations are to be expected. The recommended model for the investigation may be accepted since there is little to no difference between the stresses in the two models.

In the Figs. 11 and 12, you can see how the two models' results for stress vary from one another. The rubber concrete model shows higher stresses than the control slab model at slab lengths below 4.5 meters, whereas the SFRC concrete model shows lower stresses. The load transfer mechanism, which helps to reduce stresses brought on by the central slab by redistributing some of them to the adjacent slabs, is responsible for this variation. The results graph makes it evident that the stress is the same for all lengths equal to or more than 4.5 meters (Fig. 12).

5. Conclusion

The supplied models can capture the load-displacement behavior of fracture mechanics models, and the numerical results of tire load analysis show that the first model can mimic the behavior of other models. The purpose of this study is to analyze the effects of load and subgrade modulus on the behavior of concrete pavement. The following issues can be inferred from the present work:

1. Research proves that both models can accurately forecast the shear stress and displacement histories of a concrete pavement subject to tire contact. It gives a rough idea of where the crack first started, capturing the magnitude of the resulting force's history. Due to the restricted crack routes, it is unable to predict fracture propagation.

2. An examination of the differences between concrete pavement, CR-reinforced concrete pavement, SFRC concrete, and CR-SFRC concrete is the main contribution of this paper.

3. The model of combining SFRC with rubber as an additives to the concrete shows more promise as it more precisely represents the aging quantity of concrete pavement and the structural reaction to displacements. There are a lot of benefits from a practical standpoint. The convergence of the FE analysis is improved, on the one hand, by the availability of the explicit form of the constitutive law and the tangent matrix. The ability to see different failure modes is made possible, however, by the direct manipulation of different types of fracture stresses. Faulty components need not be fixed in advance. This section discusses the method's successes and current efforts to fill knowledge gaps. This article provides a detailed breakdown of the procedures and parameters necessary to run an ANSYS analysis on a reinforced concrete pavement case study.

4. According to the FE analytical experiments conducted on the six investigated cases, the displacement re-

sponse and tire behavior in concrete pavements are in extremely good agreement.

5. The optimal enchainment was reached when crumb rubber fiber (10%) SFRC (60%) was introduced to concrete pavement concrete with a high load impact. Increasing the number of steel fibers per cubic meter of concrete increases the interlocking process that the fibers will overlap. As the amount of fiber increased, the generated stresses in the concrete were effectively controlled by this group of overlapping fiber. There is exceptional contact between the fiber and the adjacent concrete, which significantly facilitates the process of tension.

List of Abbreviations.

Abbreviation	Full Form
SFRC	Steel Fibre Reinforced Concrete
PET	Polyethylene Terephthalate
LDPE	Low-Thickness Polyethylene
HSC	High Strength Concrete
FRC	Fibre-Reinforced Concrete
FEM	Finite Element Method
ASTM	American Society for Testing and Materials

References

[1] M. Tagba, S. Li, M. Jiang, X. Gao, M. L. Benmalek, S. Boukour, and C. Liu, (2021) *"Performance Evaluation of Cementitious Composites Containing Granulated Rubber Wastes, Silica Fume, and Blast Furnace Slag"* **Crystals *11***(6): 632.

[2] B. H. Al-Humeidawi, (2014) *"Utilization of waste plastic and recycle concrete aggregate in production of hot mix asphalt"* **Al-Qadisiyah Journal for Engineering Sciences *7***(4): 322–330.

[3] G. Li, M. A. Stubblefield, G. Garrick, J. Eggers, C. Abadie, and B. Huang, (2004) *"Development of waste tire modified concrete"* **Cement and Concrete Research *34***(12): 2283–2289.

[4] O. Y. Marzouk, R. Dheilly, and M. Queneudec, (2007) *"Valorization of post-consumer waste plastic in cementitious concrete composites"* **Waste management *27***(2): 310–318.

[5] A. Benazzouk and M. Queneudec. "Durability of cement-rubber composites under freeze thaw cycles". In: *Proceeding of International congress of Sustainable Concrete Construction, Dundee-Scotland*. 2002, 355–362.

[6] K. A. Paine, R. Dhir, R. Moroney, and K. Kopasakis. "Use of crumb rubber to achieve freeze thaw resisting concrete". In: *Proceedings of the International Conference on Concrete for Extreme Conditions, University of Dundee, Scotland, UK*. 2002, 486–498.

[7] B. Z. Savas, S. Ahmad, and D. Fedroff, (1997) *"Freeze-thaw durability of concrete with ground waste tire rubber"* **Transportation Research Record *1574***(1): 80–88.

[8] F. Hernández-Olivares and G. Barluenga, (2004) *"Fire performance of recycled rubber-filled high-strength concrete"* **Cement and concrete research *34***(1): 109–117.

[9] S. Yang, B. H. Kjartanson, and R. A. Lohnes, (2001) *"Structural performance of scrap tire culverts"* **Canadian Journal of Civil Engineering *28***(2): 179–189.

[10] L. AYADI, (2015) *"CHAMBRE SYNDICALE NATIONALE DES GROSSISTES IMPORTATEURS DE PNEUMATIQUES"*:

[11] A. Elghazouli, D. Bompa, B. Xu, A. Ruiz-Teran, and P. Stafford, (2018) *"Performance of rubberised reinforced concrete members under cyclic loading"* **Engineering Structures *166***: 526–545.

[12] N. Tangboriboon, P. Phudkrachang, L.-o. Mulsow, W. Kunchornsup, and A. Sirivat, (2013) *"Removal of water extractable proteins from concentrated natural rubber latex by eggshells"* **Journal of Elastomers & Plastics *45***(3): 253–269.

[13] P. E. Sebaaly, V. T. Gopal, and M. Ardila-Coulson. *Impact of Crumb Rubber and Other Fillers on the Rheological Properties of Binders*. Tech. rep. 2000.

[14] D. Yerezhep, A. Tychengulova, D. Sokolov, and A. Aldiyarov, (2021) *"A multifaceted approach for cryogenic waste tire recycling"* **Polymers *13***(15): 2494.

[15] M. Myhre, S. Saiwari, W. Dierkes, and J. Noordermeer, (2012) *"Rubber recycling: chemistry, processing, and applications"* **Rubber chemistry and technology *85***(3): 408–449.

[16] A. Isayev and J. Oh, (2005) *"Tire Materials: Recovery and Re-use"* **The Pneumatic Tire *18***: 670–691.

[17] W. K. Dierkes, K. Dijkhuis, H. v. Hoek, J. Noordermeer, L. Reuvekamp, S. Saiwari, and A. Blume, (2019) *"Designing of cradle-to-cradle loops for elastomer products"* **Plastics, Rubber and Composites *48***(1): 3–13.

[18] A. Macsiniuc, A. Rochette, and D. Rodrigue, (2013) *"Effect of SBR rubber particle size distribution on its thermo-mechano-chemical regeneration"* **Progress in Rubber Plastics and Recycling Technology *29***(4): 217–238.

[19] S. Saiwari, J. W. Van Hoek, W. K. Dierkes, L. E. Reuvekamp, G. Heideman, A. Blume, and J. W. Noordermeer, (2016) *"Upscaling of a batch de-vulcanization process for ground car tire rubber to a continuous process in a twin screw extruder"* **Materials** ***9***(9): 724.

[20] I. Löfgren, (2005) *"Fibre-reinforced concrete for industrial construction"* **Göteborg: Chalmers**:

[21] C. Aire, C. Mendoza, and P. Davila. "Polypropylene fibers reinforced concrete: Optimization on plastic shrinkage cracking". In: *Proceedings of the Second International Conference on Future Concrete, Abu Dhabi, United Arab Emirates*. ***12***. 2011.

[22] A. Singh and S. Bhowmik. "Use of Plastic Waste in Bitumen". In: *Smart Cities and Machine Learning in Urban Health*. Ed. by J. Thomas, V. Geropanta, A. Karagianni, V. Panchenko, and P. Vasant. IGI Global, 2022, 156–188. DOI: 10.4018/978-1-7998-7176-7.ch008.

[23] M. A. H. Al-Jumaili. "Sustainability of asphalt paving materials containing different waste materials". In: *IOP Conference Series: Materials Science and Engineering*. ***454***. 1. IOP Publishing. 2018, 012176.

[24] M. Di Prisco, G. Plizzari, and L. Vandewalle, (2009) *"Fibre reinforced concrete: new design perspectives"* **Materials and structures** ***42***: 1261–1281.

[25] J. C. Walraven, (2009) *"High performance fiber reinforced concrete: progress in knowledge and design codes"* **Materials and Structures** ***42***(9): 1247.

[26] A. De la Fuente, P. Pujadas, A. Blanco, and A. Aguado, (2012) *"Experiences in Barcelona with the use of fibres in segmental linings"* **Tunnelling and Underground Space Technology** ***27***(1): 60–71.

[27] L. Liao, A. de la Fuente, S. Cavalaro, and A. Aguado, (2015) *"Design of FRC tunnel segments considering the ductility requirements of the Model Code 2010"* **Tunnelling and Underground Space Technology** ***47***: 200–210.

[28] S. L. Suhaendi and T. Horiguchi, (2005) *"Fiber-reinforced high-strength concrete under elevated temperature-effect of fibers on residual properties"* **Fire Safety Science** ***8***: 271–278.

[29] Z. Li, M. Wu, J. Wu, Y. Cui, and X. Xue, (2020) *"Steel fibre reinforced concrete meso-scale numerical analysis"* **Advances in Civil Engineering** ***2020***: 1–16.

[30] G. Batson, (1976) *"Steel fiber reinforced concrete"* **Materials Science and Engineering** ***25***: 53–58.

[31] W. Bu, (2008) *"Punching shear retrofit method using shear bolts for reinforced concrete slabs under seismic loading"*:

[32] J. E. Shoenberger and J. G. Tom. *Polypropylene Fibers in Portland Cement Concrete Pavements.* Tech. rep. ARMY ENGINEER WATERWAYS EXPERIMENT STATION VICKSBURG MS GEOTECHNICAL LAB, 1992.

[33] Y. Singh, S. Singh, and H. Singh. "Effect of Steel Fibers on the Sorptivity of Concrete". In: *Fatigue, Durability, and Fracture Mechanics: Proceedings of Fatigue Durability India 2019*. Springer. 2021, 479–491.

[34] Z. I. Khayoun, H. M. Kamal, and Y. K. Ibrahim, (2020) *"The effect of hybrid fibers reinforcement on the mechanical and physical properties of concrete"* **The Open Civil Engineering Journal** ***14***(1):